

Characterization of ionic conduction and electrode polarization relaxation processes in ethylene glycol oligomers

R J Sengwa (✉) and Sonu Sankhla

Dielectric Research Laboratory, Department of Physics,
J N V University, Jodhpur – 342 005, India
E-mail: rjsengwa@rediffmail.com

Received: 23 May 2007 / Revised version: 2 August 2007 / Accepted: 26 December 2007
Published online: 19 January 2008 – © Springer-Verlag 2008

Summary

The complex relative dielectric function, dielectric loss tangent, electric modulus, alternating current electrical conductivity and impedance spectra of ethylene glycol oligomers (EGOs) i.e., ethylene glycol, diethylene glycol and poly(ethylene glycol)s of average molecular weight 200, 300, 400 and 600 g mol⁻¹ have been investigated in the frequency range 20 Hz to 1 MHz at 25°C. These EGOs show the low frequency dielectric/electrical dispersion due to electrode polarization and ionic conduction effects. The ‘master curves representation’ of the real and imaginary parts of the intensive dielectric/electrical functions were used to evaluate the relaxation times corresponding to these effects processes. The comparative dielectric study of EGOs confirms that the values of low frequency relaxation times and direct current electrical conductivity are influenced by the chain flexibility and its random coiling.

Introduction

Advancement in dielectric measurements has made the broadband dielectric spectroscopy expand over the frequency range varying from μHz to THz [1]. In polar liquids, the low frequency dielectric dispersion occurs due to the ionic conduction and electrode polarization phenomena [1-5], whereas the high frequency dielectric dispersion corresponds to the molecular reorientation dynamics and the intramolecular group rotations [6-8]. The conformation of the formation of molecular network structures through hydrogen bonds in the hydroxyl group (–OH) containing polar liquids have been the subject of several investigations since the initial stage of dielectric spectroscopy [9,10]. The molecules of ethylene glycol oligomers (EGOs) have ends –OH groups, which form complexes with different materials through hydrogen bonds. Due to the H–bond compatibility of EGOs, they being biocompatible have a wide range of biological [11] and electrochemical applications [12-14]. Shinyashiki *et al* [2,15,16], Sato *et al* [17] and Sengwa *et al* [18,19] have extensively investigated the mixtures of EGOs in different non-polar, polar and polymeric systems in order to get the information on the heterogeneous molecular interactions, molecular dynamics and their structures. The microwave dielectric relaxation behaviour of pure

EGOs were also investigated by the author in the frequency range 200 MHz – 20 GHz to confirm the chain flexibility and coiling with increasing molecular chainlength, and its effect on the dielectric constant and molecular reorientation relaxation time [20].

The existence of free ions in liquid polar dielectric is very common, which is the main reason of the occurrence of low frequency dielectric dispersion [1-5]. Further, the electrode polarization (EP) is also one of the most undesired effect in low frequency dielectric spectroscopy, which occurs due to blocking of charges at the sample/electrode interface [1-5,14,21]. In the present paper, an attempt has been made to characterize the comparative dielectric/electrical behaviour of EGOs in regard to ionic and EP phenomena and corresponding relaxation times in the frequency range 20 Hz to 1 MHz at 25°C. Further, these relaxation times were also correlated with the high frequency molecular reorientation dielectric relaxation time of these systems.

Experimental

Materials

Grade reagent of ethylene glycol oligomers (EGOs) [$\text{H}-(\text{O}-\text{CH}_2-\text{CH}_2)_n-\text{OH}$] namely ethylene glycol (EG), diethylene glycol (DEG), and poly(ethylene glycol)s (PEGs) of average molecular weight 200, 300, 400 and 600 g mol⁻¹ (PEG200, PEG300, PEG400 and PEG600) were purchased from Loba Chemie, India.

Dielectric measurements

An Agilent 4284A Precision LCR Meter and a four terminal nickel-plated cobal (an alloy of 17% Cobalt + 29% Nickel + 54% Iron) electrode dielectric cell Agilent 16452A Liquid Test Fixture were used for the capacitance and resistance measurement in the frequency range 20 Hz to 1 MHz. The short circuit compensation technique was used to calibrate the liquid dielectric test fixture before the sample measurements. The test fixture correction coefficient was also considered to cancel the effect of stray capacitance during the evaluation of the values of complex relative dielectric function. All measurements were made at 25°C and the temperature was controlled by Thermo-Haake DC10 controller with a precision of $\pm 0.01^\circ\text{C}$.

The complex relative dielectric function $\epsilon^*(\omega)$ is determined from the relation [22]

$$\epsilon^*(\omega) = \epsilon' - j\epsilon'' = \alpha \left(\frac{C_p}{C_o} - j \frac{1}{\omega C_o R_p} \right) \quad (1)$$

where $\omega = 2\pi f$ is the angular frequency, C_o and C_p are the measured values of the capacitances of the dielectric cell without and with sample, respectively, R_p is the equivalent parallel resistance of the cell with sample, and α is the correction coefficient of the cell.

Data analysis and results

Figures 1–6 show the spectra of the real part of relative dielectric function ϵ' , dielectric loss ϵ'' , and loss tangent $\tan\delta = \epsilon''/\epsilon'$ of the EG, DEG, PEG200, PEG300, PEG400 and PEG600, respectively at 25°C. The complex alternating current (ac) conductivity, $\sigma^*(\omega)$ of the EGOs were obtained from the relation

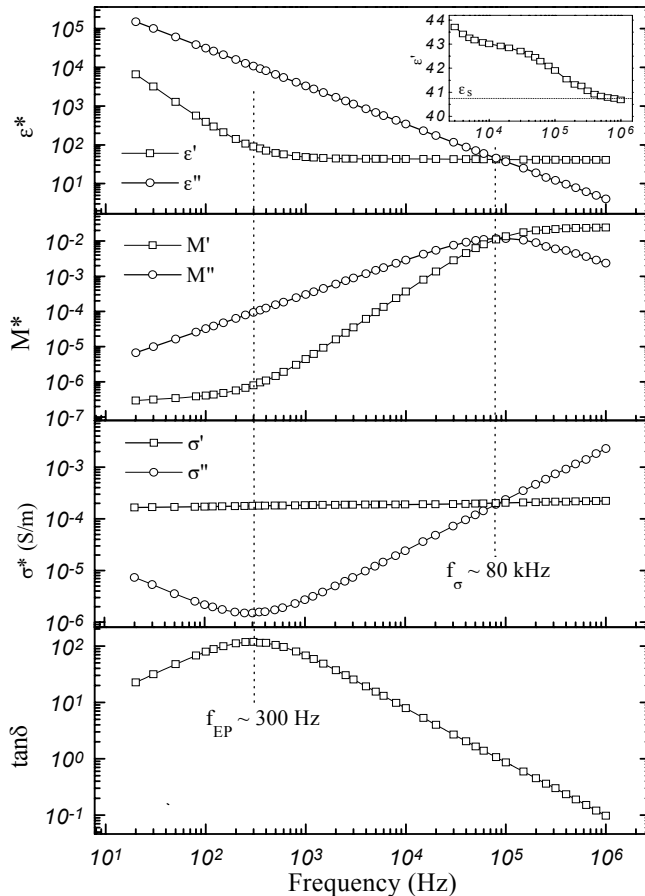


Figure 1. Simultaneous superpositions of the frequency dependent real and imaginary parts spectra of ϵ^* , M^* and σ^* along with $\tan\delta$ of EG at 25°C.

$$\sigma^*(\omega) = \sigma' + j\sigma'' = j\omega\epsilon_0\epsilon^*(\omega) = \omega\epsilon_0\epsilon'' + j\omega\epsilon_0\epsilon' \quad (2)$$

where ϵ_0 (8.854×10^{-12} F/m) is the dielectric constant of vacuum. The conductivity spectra of the EGOs at 25°C are shown in Figures 1–6.

Considering the charges as the independent variable, conductivity relaxation effects can be suitably analyzed within the electric modulus formalism in terms of a dimensionless quantity, $M^*(\omega)$. Analogous to mechanical relaxation, the electric modulus $M^*(\omega)$ is obtained from the relation [23]

$$M^*(\omega) = \frac{1}{\epsilon^*(\omega)} = M' + jM'' = \frac{\epsilon'}{\epsilon'^2 + \epsilon''^2} + j\frac{\epsilon''}{\epsilon'^2 + \epsilon''^2} \quad (3)$$

The main advantage of this formulation is that, the space charge effects often do not mask the features of the spectra, owing to the suppression of high capacitance phenomena in $M''(f)$ plots.

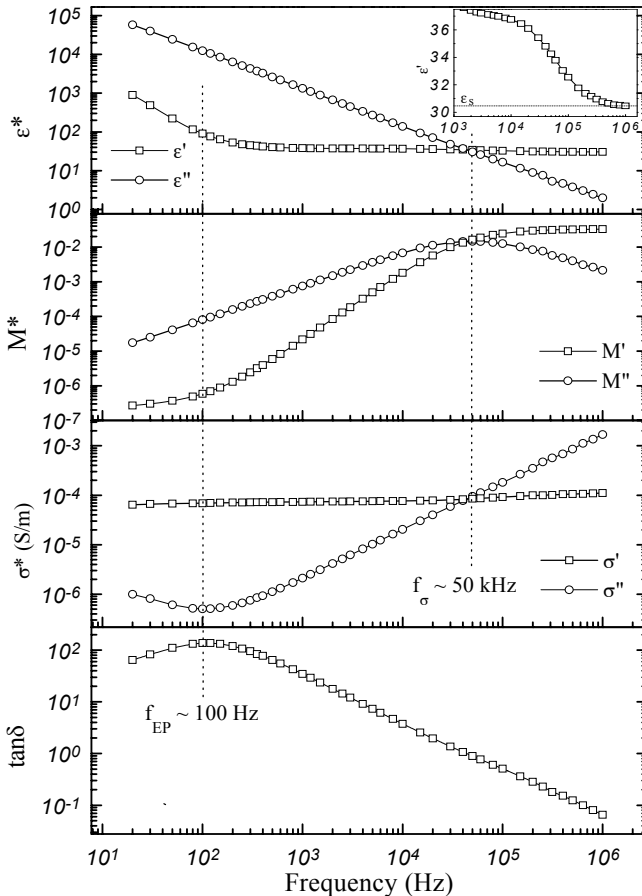


Figure 2. Simultaneous superpositions of the frequency dependent real and imaginary parts spectra of ϵ^* , M^* and σ^* along with $\tan\delta$ of DEG at 25°C.

The M' and M'' values evaluated from Eq. 3 for the EGOs at 25°C, are also plotted against frequency in Figures 1–6. The $M''(f)$ spectra of these materials have a peak, and the frequency (denoted by f_σ) corresponding to it is related to the ionic conductivity relaxation, where both charge carrier transport and reorientation may contribute to the electric field relaxation. The electrical modulus in terms of most probable ionic conduction relaxation time τ_σ can be written as [24]

$$M^*(\omega) = M_\infty \frac{j\omega\tau_\sigma}{1 + j\omega\tau_\sigma} = \frac{1}{\epsilon_\infty} \left[\frac{(\omega\tau_\sigma)^2}{1 + (\omega\tau_\sigma)^2} + j \frac{(\omega\tau_\sigma)}{1 + (\omega\tau_\sigma)^2} \right] \quad (4)$$

where ϵ_∞ is the relaxed high frequency dielectric permittivity of the liquid. From Eq. 4, $M' = M''$ at $\omega_\sigma = 2\pi f_\sigma = 1/\tau_\sigma$, where M'' also has a local maximum. Therefore, the τ_σ values were obtained directly from the value of frequency f_σ corresponding to the peak of $M''(f)$ spectrum [4,5,24]. The $M''(f)$ data were fit using the Origin® nonlinear curve fitting tool to find the correct value of f_σ .

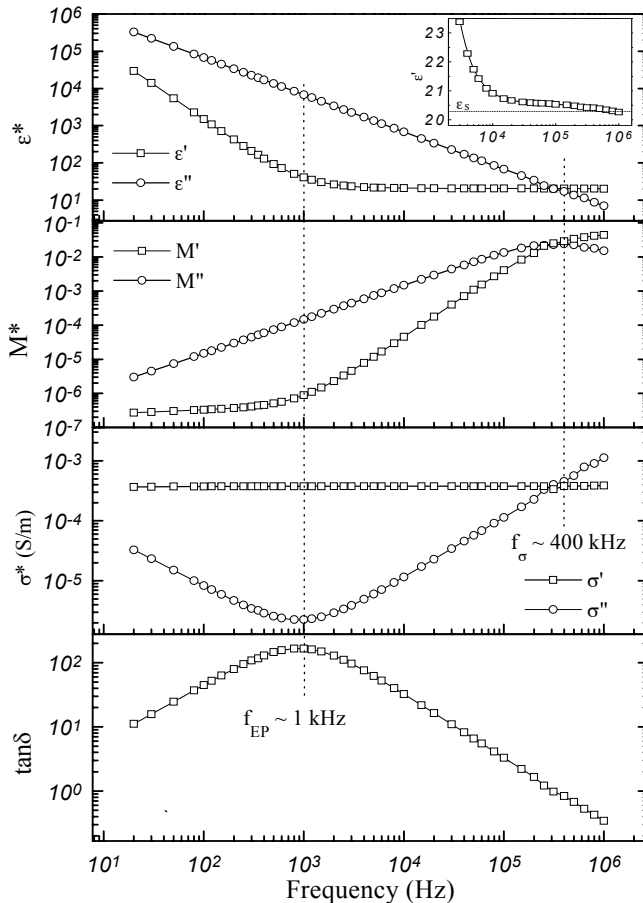


Figure 3. Simultaneous superpositions of the frequency dependent real and imaginary parts spectra of ϵ^* , M^* and σ^* , along with $\tan\delta$ of PEG200 at 25°C.

The simultaneous plots of the frequency dependent spectra of the real and imaginary parts of the intensive quantities ϵ^* , M^* and σ^* , along with $\tan\delta$ are called ‘master curve representation’. The strong upturn of ϵ' at low frequency in Figures 1–6 arises from the accumulation of ions at the electrode interface, i.e., the so-called electrode polarization (EP) effect. From the master curves, it can be seen that the $\tan\delta$ peak frequency f_{EP} value is closely related with the frequency corresponding to the strong upturn of the ϵ' values. Therefore the values of electrode polarization relaxation time τ_{EP} in case of EGOs were determined from the relation $\tau_{EP} = 1/(2\pi f_{EP})$, which involves charging/discharging of the electrode double layer capacitance [3–5,21]. The exact value of f_{EP} is determined by fitting the $\tan\delta(f)$ data to the Origin® nonlinear curve fitting tool.

The complex impedance formalism $Z^*(\omega)$ is commonly used to separate the bulk (dielectric sample) and the electrode surface phenomena [3–5,25–27]. A common feature of dielectrics with *dc* conductivity σ_0 is a discontinuity at electrode/dielectric interface, which has different polarization properties than the bulk dielectric.

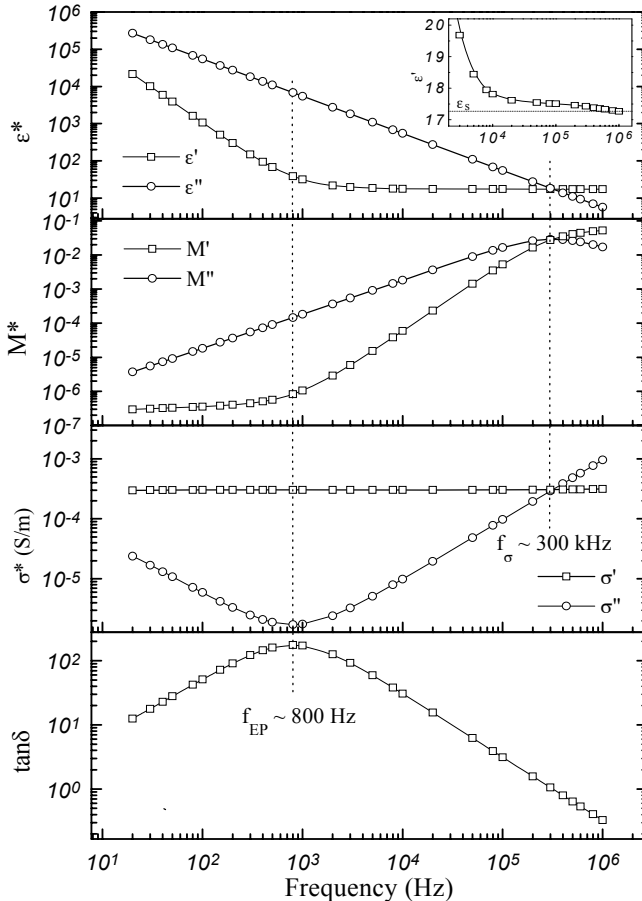


Figure 4. Simultaneous superpositions of the frequency dependent real and imaginary parts spectra of ϵ^* , M^* and σ^* along with $\tan\delta$ of PEG300 at 25°C.

The complex impedance $Z^*(\omega)$ of the EGOs were evaluated by the relation

$$Z^*(\omega) = \frac{1}{Y^*(\omega)} = Z' - jZ'' = \frac{R_p}{1 + (\omega C_p R_p)^2} - j \frac{\omega C_p R_p^2}{1 + (\omega C_p R_p)^2} \quad (5)$$

The complex impedance plane plots (Z'' vs. Z') for the EG, DEG, PEG200, PEG300, PEG400 and PEG600 are plotted in Figure 7 to determine the values of f_{EP} from the impedance plots technique, which separates the bulk and the electrode polarization phenomena [3-5,25-27]. In these impedance plots the frequency of the experimental points increases on going from right to left side on the arcs. The appearance of two separate arcs in these plots corresponds to the bulk effect (the high frequency arc), and the electrode surface polarization (EP) effect (the low-frequency arc) as indicated in Figure 7. The value of f_{EP} corresponding to Z'' minimum, as indicated in respective plots of Figure 7, separates the bulk effect and the electrode surface effect [3-5,25-27].

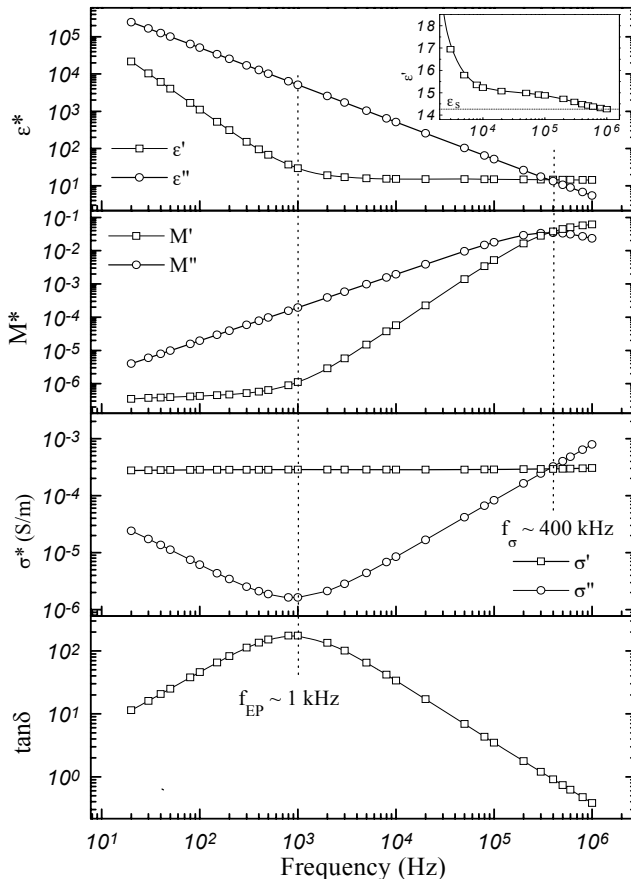


Figure 5. Simultaneous superpositions of the frequency dependent real and imaginary parts spectra of ϵ^* , M^* and σ^* along with $\tan\delta$ of PEG400 at 25°C.

Figure 7 shows that these f_{EP} values of different EGOs are exactly equal to the frequency values of $\tan\delta$ peak f_{EP} , as indicated in the respective EGOs ‘master curve representation’ (Figures 1–6). The values of dc resistance R_{dc} of the EGOs were determined from the extrapolated intercept value on the real impedance axis Z' of the common point of the bulk and EP arcs [3,4,27], which is also indicated by vertical dotted lines on each EGO impedance plot of Figure 7.

The evaluated values of the τ_σ , τ_{EP} , σ_o and R_{dc} for EG, DEG, PEG200, PEG300, PEG400 and PEG600 at 25°C alongwith other dielectric parameters [18,20] are shown in Table 1. Further, these values are also plotted against the average number of EGOs monomer units n in Figure 8.

Discussion

Behaviour of master curves representation

Comparative shape and magnitude study of the ‘master curve representation’ spectra of the intensive quantities $\epsilon^*(\omega)$, $M^*(\omega)$ and $\sigma^*(\omega)$ of the studied EGOs (Figures 1–6)

suggest that the low frequency dielectric dispersion of these liquids varies anomalously with the increase in their molecular chain. The frequency dependent ϵ'' values of these liquids decreases with the increase in frequency and the magnitude of ϵ'' has the order PEG200 > PEG300 > PEG400 > EG > PEG600 > DEG.

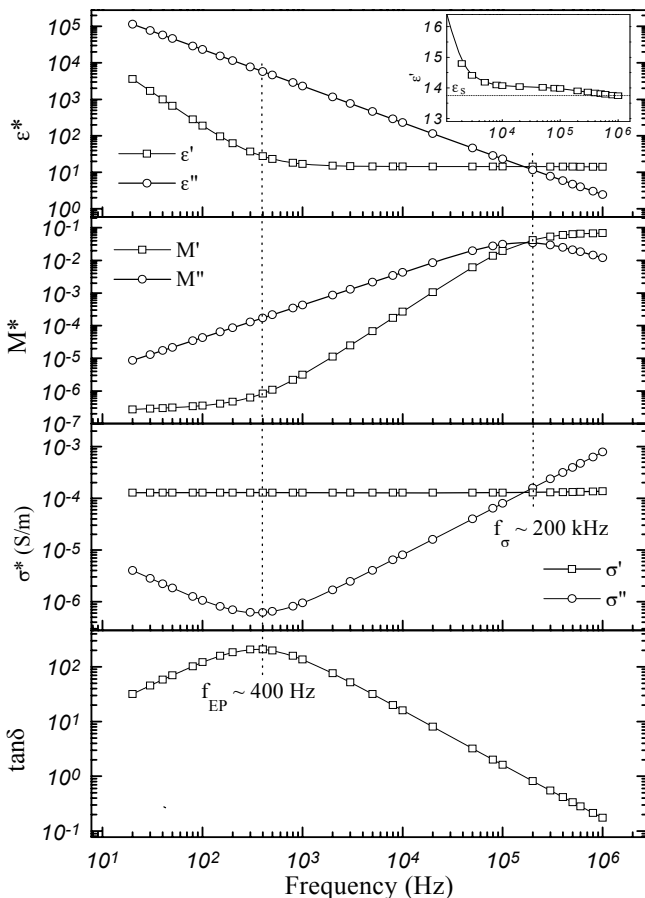


Figure 6. Simultaneous superpositions of the frequency dependent real and imaginary parts spectra of ϵ^* , M^* and σ^* along with $\tan\delta$ of PEG600 at 25°C.

The ϵ' values of the EGOs gradually approaches their static permittivity ϵ_s values as the frequency exceeds 100 kHz, which is shown in the insets of Figures 1–6. The ϵ_s values of the EGOs decreases with increase of n , which is the characteristic behaviour of the homologous series. The decrease in ϵ_s values is mainly due to the increase in the number of carbon atoms in the EGOs molecular chain. From Table 1, we can see that the ϵ_s values approaches a limiting value for higher n value EGOs molecules. Earlier [2], it is confirmed that the broadband dielectric spectra of the solutions of the polymer–solvent blends can be well described by a sum of three dielectric relaxation processes with the contribution of *dc* conductivity. The low-frequency process is

caused by the electrode polarization and ionic conduction phenomena [2-5], whereas the middle frequency process corresponds to the micro-Brownian motion of the polymer chain [2,4,5]. The high frequency process corresponds to the reorientation motion of small-size polar molecules used as solvent for the polymer solutions, which occurs in the microwave frequency region [2,15-17,19,20].

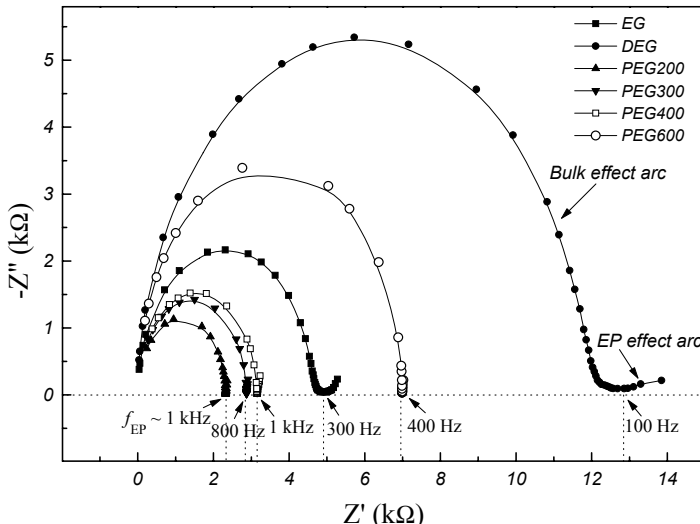


Figure 7. Complex impedance plane plots (Z'' vs. Z') for the EGOs at 25°C.

The approach of the low-frequency dispersion ϵ' values of EGOs to their ϵ_s values around 1 MHz frequency in the present study and the earlier high frequency dispersion study [20], confirms that the pure EGOs molecules have no dispersion corresponding to their segmental motion i.e. middle frequency process (m -process) [2]. But in case of polymers-EGOs blends [2,4,5], the m -process is observed in MHz frequency region, which is influenced by the polymer concentration and the size of EGOs in the blend. Further the chain flexibility and random coiling significantly affects the high frequency process of the EGOs molecules [20].

Table 1. Values of the average number of monomer units n , static dielectric constant ϵ_s , dipole moment μ in non-polar solvent, specific dipole moment μ_{sp} , Kirkwood correlation factor g , molecular reorientation relaxation time τ , ionic conductivity relaxation time τ_σ , electrode polarization relaxation time τ_{EP} , dc electrical conductivity σ_0 and dc resistance R_{dc} of ethylene glycol oligomers (EGOs) at 25°C

EGOs	n	ϵ_s	μ (D)	μ_{sp} (D)	g	τ (ps)	τ_σ (μs)	τ_{EP} (ms)	$\sigma_0 \times 10^4$ (S/m)	R_{dc} (kΩ)
EG	1	40.68	2.38	2.38	2.37	92.4	1.99	0.53	1.8	4.94
DEG	2	30.47	2.69	1.90	2.26	131.8	3.18	1.59	0.71	12.86
PEG200	4.1	20.26	3.28	1.62	1.81	122.8	0.38	0.16	3.7	2.32
PEG300	6.4	17.26	3.91	1.55	1.61	97.5	0.53	0.20	3.0	2.87
PEG400	8.7	14.27	4.20	1.42	1.50	129.2	0.38	0.16	2.8	3.15
PEG600	13.2	13.74	4.82	1.33	1.64	75.8	0.79	0.39	1.3	6.99

Values of μ , g and τ [Refs. 18, 20]

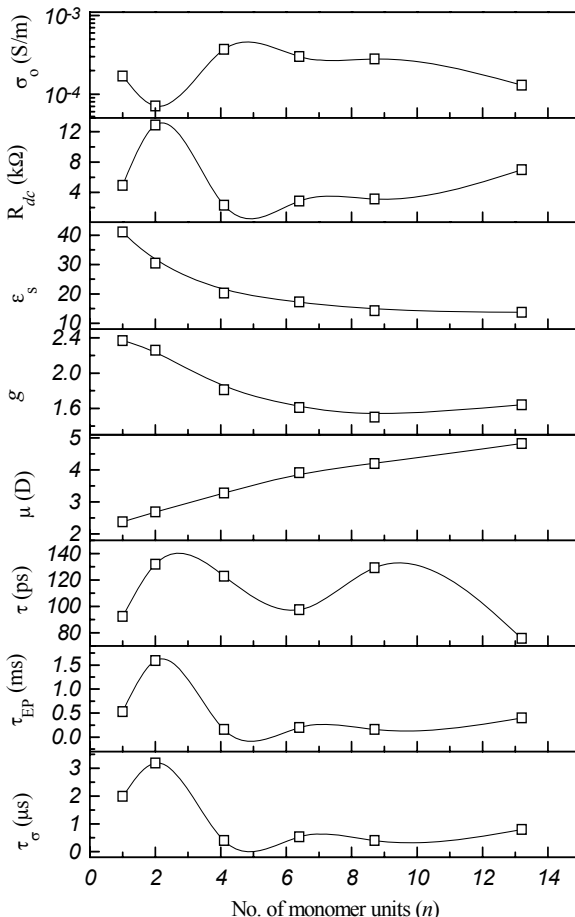


Figure 8. Plots of various dielectric parameters as a function of the average number of monomer units n of EGOs at 25°C.

The real part of electric modulus M' of the EGOs have the dispersion in the frequency range from f_{EP} to the f_σ (Figures 1–6). Further the f_σ value has the shift towards lower frequency region for DEG as compared to EG, but there is an abrupt increase in its value for $n > 2$, which also shows anomalous behaviour.

The conductivity plots show that the σ' values have the plateaus in the frequency region below the f_σ which corresponds to the dc conductivity σ_0 value, whereas above it the σ' value slowly increases (Figures 1–6). Figure 8 shows that the σ_0 value of DEG is lower than EG, which reflects the comparatively low short-range motion of DEG molecules. The large rise in σ_0 value for the EGOs of $n > 2$ is mainly due to the increase in their chain flexibility but it seems that the chain coiling reduces the σ_0 values. The R_{dc} values of the EGOs clearly show the inverse behaviour as compared to the σ_0 values with the increase of n value (Table 1, Figure 8).

The tan δ peak, which corresponds to f_{EP} value also varies anomalously with increase in molecular chain of EGOs. Further tan δ peak magnitude is found ~ 100 for these liquid EGOs (Figures 1–6). Earlier [3–5] in case of polymers solution and their blends

in polar solvent, the value of $\tan\delta$ peak is also found ~ 100 for the same dielectric test fixture. These comparative results confirm that the magnitude of $\tan\delta$ peak, which is related to the electrode polarization phenomena, is independent of the liquid dielectric sample but strongly depends on the electrode material of the sample holder. Further, the impedance plots (Figure 7) shows that the EP effect arc of DEG spreads more as compared to the EG. But in case of flexible chain EGOs the EP effect arcs are narrower to the bulk effect arcs (Figure 7).

Dielectric relaxation behaviour

Earlier [20], from microwave dielectric relaxation study, it is observed that the value of molecular reorientation relaxation time τ of these EGOs molecules varies anomalously with increase in the degree of polymerization (Table 1). But their dipole moment μ values increases almost linearly with increase of n value (Figure 8), and the specific dipole moment μ_{sp} ($\mu_{sp} = (\mu^2 / n)^{1/2}$) approaches a limiting value for higher n value EGOs (Table 1). The values of Kirkwood correlation factor g [16] (Table 1) for these molecules, which is a measure of the short-range intermolecular association strength, decreases with the increase in monomer units of EGOs. The decreases of g values show that the intermolecular ordering range of the parallel dipolar alignment decreases and approaches almost a constant value with increasing molecular size for higher EGOs molecules. In general, τ values of small size associating molecules of the homologous series are governed by their molecular size and the strength of self-association (g value) [29]. But in case of EGOs the chain flexibility and its random coiling mask the effect of molecular size and molecular association (g values) which affects the τ values of EGOs having $n > 2$ [20].

Figure 8 and Table 1 shows that the τ_σ and τ_{EP} values of the lower size EGOs vary anomalously similar to their τ values with the increase of n [20]. Further, the τ_{EP} values are about three-order scale higher than the corresponding τ_σ values of the EGOs. The large increase of the τ_{EP} value of DEG as compared to the EG indicates the increase of thickness of the electric double layer formed on the electrodes surfaces [3-5,30], which takes longer time in the charging/discharging of the electric double layer capacitances. The thickness of electrode surface barrier layers arises because of the adsorption of the dielectric molecules on the electrode surfaces [30], which increases for DEG as compared to the EG. The anomalous variation in τ_{EP} values with the increase of n values of the EGOs also favours the anomalous variation of the R_{dc} values (Table 1). Further, the increase of the τ_σ value of DEG suggests that the short-range movement of the DEG molecules is more hindered as compared to higher molecular weight EGOs.

Conclusions

This paper reports the comparative values of the precisely measured dielectric/electrical spectra of ethylene glycol, diethylene glycol, PEG200, PEG300, PEG400 and PEG600 in their liquid state in the frequency range from 20 Hz to 1 MHz at 25°C. The low frequency dielectric relaxation times and the high frequency relaxation processes of the EGOs are mainly governed by the molecular chain flexibility and its random coiling. The EGOs of flexible chain of $n > 2$ have comparative different dielectric/electrical behaviour as compared to the rigid chain molecules e.g., EG and

DEG of the homologous series. Results indicates that the comparative low frequency dielectric characterization of these liquid polar dielectrics will be helpful to enhance their industrial and technological applications [12,13].

Acknowledgements. The work was done as a part of the Project No. SR/S2/CMP-9/2002 financed by the Department of Science and Technology, New Delhi, India.

References

1. Kremer F, Schonhals A (Eds) (2003) Broadband Dielectric Spectroscopy. Springer, New York
2. Shinyashiki N, Sengwa RJ, Tsubotani S, Nakamura H, Sudo S, Yagihara S (2006) *J Phys Chem A* 110:4953
3. Sengwa RJ, Sankhla S (2007) *Polymer* 48:2737
4. Sengwa RJ, Sankhla S (2007) *J Macromolecular Sci: Part B: Phys* 46:717
5. Sengwa RJ, Sankhla S (2007) *Colloid Polym Sci* 285:1237
6. Sengwa RJ, Choudhary R, Mehrotra SC (2001) *Molec Phys* 99:1805
7. Sengwa RJ, Abhilasha, More NM, Mehrotra SC (2005) *J Polym Sci: Part B: Polym Phys* 43:1134
8. Sengwa RJ, Chaudhary R, Mehrotra SC (2002) *Polymer* 43:1467
9. Smyth CP (1955) Dielectric Behaviour and Structure. McGraw-Hill, New York
10. Hill NE, Vaughan WE, Price AH, Davies M (1968) Dielectric Properties and Molecular Behaviour. Van Nostrand Reinhold Co, London
11. Harris JM, Zalipsky S (1997) Poly(ethylene glycol) Chemistry and Biological Applications. ACS Symp Ser 680, American Chemical Society, Washington DC
12. Gray FM (1997) Polymer Electrolytes. The Royal Society of Chemistry, Letchworth, HN
13. Nazri G, Pistoia G (Eds) (2004) Lithium Batteries: Science and Technology. Kluwer Academic, Boston
14. Dou S, Zhang S, Klein RJ, Runt J, Colby RH (2006) *Chem Mater* 18:4288
15. Shinyashiki N, Sudo S, Abe W, Yagihara S (1998) *J Chem Phys* 109:9843
16. Shinyashiki N, Asaka N, Mashimo S, Yagihara S (1990) *J Chem Phys* 93:760
17. Sato T, Niwa H, Chiba A, Nozaki R (1998) *J Chem Phys* 108:4138
18. Sengwa RJ, Sankhla S (2007) *J Mol Liq* 130:119
19. Sengwa RJ (2003) *Polym Int* 52:1462
20. Sengwa RJ, Kaur K, Choudhary R (2000) *Polym Int* 49: 599
21. Klein RJ, Zhang S, Dou S, Jones BH, Colby RH, Runt J (2006) *J Chem Phys* 124:144903
22. Agilent 16452A Liquid Test Fixture – Operation and Service Manual. (2000) Agilent Technologies Ltd, Japan
23. Macedo PB, Moynihan CT, Bose R (1972) *Phys Chem Glasses* 13:171
24. Zhang S, Dou S, Colby RH, Runt J (2005) *J Non Cryst Solids* 351:2825
25. Macdonald JR (Ed) (1987) Impedance Spectroscopy-Emphasizing Solid Materials and System. New York, Wiley
26. Pissis P, Kyritsis A (1997) *Solid State Ionics* 97:105
27. Kyritsis A, Pissis P, Grammatikakis J (1995) *J Polym Sci: Part B: Polym Phys* 33:1737
28. Sengwa RJ, Madhvi, Sankhla S, Sharma S (2006) *J Sol Chem* 35:1037
29. Sengwa RJ, Madhvi, Abhilasha (2006) *J Mol Liq* 123:92
30. Craig DQM, Newton JM, Hill RM (1993) *J Mater Sci* 28:405